BIOCHIP JOURNAL, Vol. 2, No. 1, 52-59, March 2008

BCG Detection Based on a Split-Flow Microcalorimetric Biosensor for the Diagnosis of Tuberculosis

Seung-Il Yoon[1], Mi-Hwa Lim[2], Se-Chul Park[1], Jeon-Soo Shin[2] & Yong-Jun Kim[1]

[1]School of Mechanical Engineering, Yonsei University,
[2]Department of Microbiology, College of Medicine, Yonsei University
Correspondence and requests for materials should be addressed to Y.-J. Kim (yjk@yonsei.ac.kr)

Accepted 31 January 2008

Abstract

This paper proposes and demonstrates a novel microcalorimetric sensor for detecting BCG (Bacillus Calmette-Guerin). In order to eliminate additional heating structures and calibration steps, a split-flow microchannel is integrated with the microcalorimeter. The split-flow microchannel keeps the output of the microcalorimeter constantly near a zero level without any heating elements when there is no biochemical reaction. By using the split-flow microchannel, an active heating element such as a heater is no longer required. And, in order to improve the sensitivity of the microcalorimeter, a thermal sensing component, a thermopile in this case, has been fabricated on a high thermal resistivity layer, which reduces a parasitic heat transfer to the silicon substrate and makes released thermal energy concentrated to the thermopile. The characteristics of the proposed microcalorimeter were investigated by measuring the reaction heat of the biotin-streptavidin pairs. The sensitivity was measured to be 0.8 W · sec/cal. Then, a biological reaction between BCG and its antibody was detected using the proposed microcalorimeter. In order to verify the reliability of the measurement, exactly the same amount of BCG was reacted with its antibody, and the optical density was measured using an enzyme-linked immunosorbent assay as a known reference.

Keywords: Microcalorimeter, Split-flow microchannel, Biotin-streptavidin, BCG, Thermal resistivity layer

Introduction

BCG (Bacillus Calmette-Guerin) has been reported to be one of the types of mycobacterium tuberculosis that causes most cases of tuberculosis. There are several standard methods for detecting BCG such as a microscopic examination with a cell culture, ELISA (enzyme-linked immunosorbent assay), and PCR-based detection[1-3]. These methods are widely used, but generally require a one-working-day procedure for detection. Considering that the clinical progress of BCG infection is so fast and induces high mortality after a delayed treatment, a real-time detection of BCG will be very helpful toward an early treatment for a better prognosis.

Various MEMS-based biosensors have been developed based on surface plasmon resonance (SPR)[4], fluorescence[5], mechanical bending[6], and nano-materials[7] for a fast and real-time diagnosis. These MEMS-based sensors have the advantages of a small size, fast detection, and high sensitivity, although they require bulky optical instruments or need complex fabrication steps. For simpler and faster BCG detection, a MEMS-based microcalorimeter can be considered as a strong candidate. It produces an electrical potential upon detection of a release or absorption of thermal energy due to biochemical reactions[8,9]. Furthermore, it does not need any immobilization process, and can be reused with a simpler biomolecule detection process.

Most of the researches related to the microcalorimeter have focused on high sensitivity and an accurate measurement. The electrical potential is proportional to temperature differences between the hot and cold junctions of the thermopile. For higher sensitivity, it is important to maximize the temperature differences between the junctions. Thus, there have been various efforts to minimize parasitic heat transfer to a substrate in order to maximize these temperature differences[10,11]. However, the hot junctions of the previous microcalorimeters still contacted with a high-thermal-loss substrate, a thin silicon diaphragm.

To achieve an accurate measurement, the hot and cold junctions have to be set at a constant temperature before a biochemical reaction process[12]. With respect to the feasibility of the junctions to maintain a constant temperature, microcalorimeters can be classified into two types: active and passive. Although a passive type is simple to fabricate[13], most of the microcalorimeters adopt an active heating element, which can make the temperatures of both junctions the same by heating the hot junctions[14]. However, the additional heating structure makes the fabrication and

measurement process more complex.

This work demonstrates an accurate passive microcalorimeter. To improve sensitivity, a high thermal resistivity layer was used between the substrate and thermal components. For accurate measurement, the split-flow microchannel was introduced. The proposed sensor was characterized by measurement of the reaction heat of biotin-streptavidin pairs. Then, the reaction heat of BCG and its antibody, α-BCG in this case, was detected by the sensor.

Results and Discussion

The biochemical reaction between BCG and its antibody, live BCG and α-BCG from a rabbit in this case, was detected using the proposed device. A total of 14 pairs of microcalorimeter were used for the measurements.

At first, 6 μL of BCG was injected into both chambers. 3 μL of the injected BCG was applied to the reaction chamber, which included 1.0×10^5, 1.0×10^6, 1.0×10^7, 1.0×10^8, and 1.0×10^9 Colony Forming Units (CFU) of BCG. Then, 3 μL of 300 ng/μL α-BCG was applied into the reaction chamber only. Finally, output signal changes due to the biochemical reaction between BCG and α-BCG were recorded using a voltage meter.

Detection of BCG

In order to investigate the effects of the impact of biomolecule injection, BCG was injected three times before the injection of α-BCG. Insignificant changes in the output signals due to the BCG injection itself were observed when there was no biochemical reaction. But there was a noticeable signal change only when α-BCG was injected into the reaction chamber. Figure 1(a) shows the measured output voltages according to the amount of BCG. When α-BCG was injected, a peak in the output voltage changes occurred, and this change was recovered after about 20 seconds. The measurements for each amount of BCG were repeated 30 to 40 times.

The measured output voltages can be transformed into generated energies, which are called output signals, by calculating the area of the measured output voltages. The output signals according to the amount of BCG were 5.01×10^{-12}, 2.07×10^{-11}, 5.74×10^{-11}, 2.20×10^{-10}, and 5.13×10^{-10} W · sec as shown in Figure 1(b). And the reaction heats of BCG and its antibody can be calculated. The calculated reaction heats of BCG according to its amount were 1.19×10^{-12}, 4.93×10^{-11}, 1.37×10^{-11}, 5.24×10^{-11}, and 1.22×10^{-10} calories. And the reaction heats per CFU

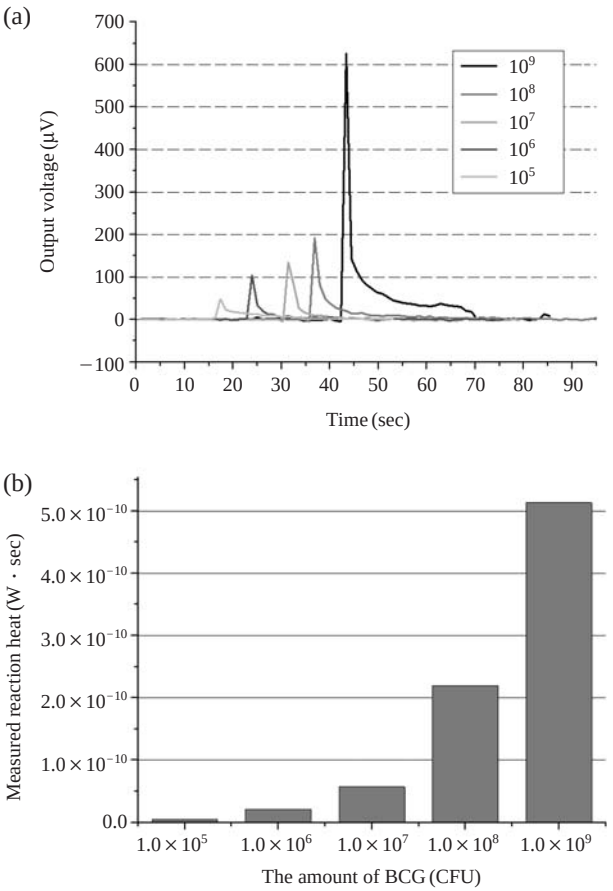

Figure 1. Results of BCG detection; (a) The measured output voltages according to the amounts of BCG, (b) the calculated output signals according to the amounts of BCG.

of BCG decreased from 1.19×10^{-17} to 1.22×10^{-119} cal/CFU as the amount of BCG increased. This means that the number of binding sites per bacteria decreases as the ratio between the injected amounts of BCG and α-BCG decreases. Table 1 lists the calculated reaction heats from the measured output voltages.

Verification of the Detection Results by the Split-flow Microcalorimeter

The measured results using the proposed microcalorimeter were verified by demonstrating several control experiments. The control experiments could be classified into two types, largely. The first type was for checking whether the output signals were originated from only the biochemical reaction. For this, the effects by a solution injection, non-specific binding, and different buffered solution were examined. And the second type was for checking the feasibility of the proposed microcalorimeter as a biosensor by

Table 1. Measured output signals and calculated reaction heats of BCG-antibody reaction according to the amounts of BCG.

The amount of BCG (CFU)	Measured output signal (W · sec)		Calculated reaction heat (cal)
	Average	Standard variation	
1.0×10^{5}	5.01×10^{-12}	2.35×10^{-16}	1.19×10^{-12}
1.0×10^{6}	2.07×10^{-11}	8.32×10^{-17}	4.93×10^{-12}
1.0×10^{7}	5.74×10^{-11}	2.79×10^{-16}	1.37×10^{-11}
1.0×10^{8}	2.20×10^{-10}	6.57×10^{-16}	5.24×10^{-11}
1.0×10^{9}	5.13×10^{-10}	4.54×10^{-14}	1.22×10^{-10}

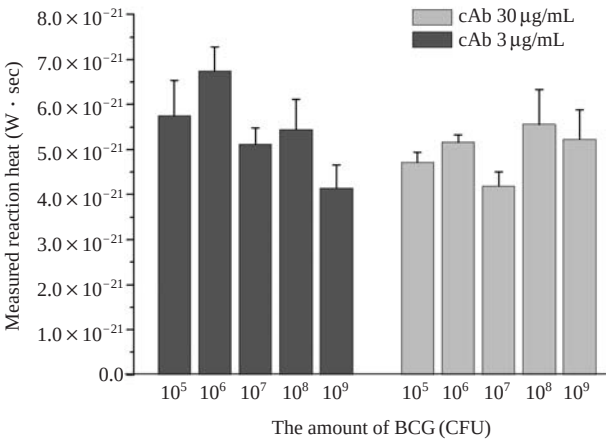

Figure 2. Results of the cases of negative control; Antibody for *E. coli* instead of BCG was used, and the measured output signals were very insignificant compared with the results of BCG detection.

comparing it with ELISA.

First of all, in order to examine the effects due to solution injections themselves and non-specific bindings, a control antibody, which is a specific antibody for *E. coli*, was used instead of α-BCG, and its resulting heat was then measured.

As shown in Figure 2, the output signal changes due to the non-specific binding and solution injection are insignificant compared with the results of BCG detection. This means that the thermal energy and considerable output voltage changes were originated from only the biochemical reaction of BCG and its antibody.

Furthermore, the BCG detection results of the proposed microcalorimeter were verified using ELISA, which is one of the most popular immunoassays. The exact same amounts of BCG were reacted with α-BCG, and the optical density was measured using ELISA. As shown in Figure 3, the two experimental results correspond well, showing the possibility of

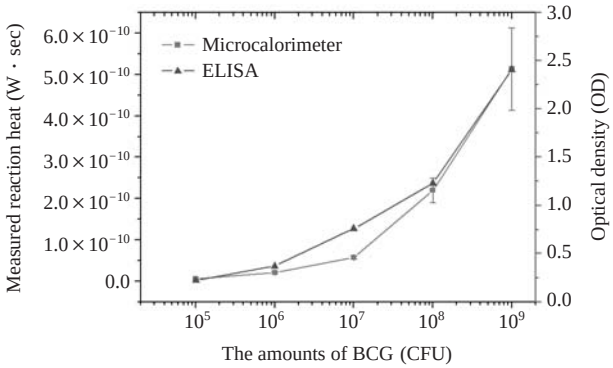

Figure 3. Comparison of results between the microcalorimeter and ELISA.

low-cost quantization of biomedical materials.

Conclusions

A novel split-flow microcalorimeter was designed and fabricated using polymer-based micromachining. Even though the proposed microcalorimeter is of a passive type without a heating structure, the output signal was maintained at a nearly zero level by using the split-flow microchannel when there was no biochemical reaction. At the same time, the split-flow microchannel reduced the measurement time because the calibration steps were eliminated. The thermal sensing component was fabricated on a high thermal resistivity layer to improve sensitivity. The split-flow microcalorimeter was characterized by measuring the reaction heat of biotin-streptavidin pairs. Its sensitivity was 0.8 W · sec/cal. After its characterization, BCG of various amounts was detected. The measured reaction heats of BCG and its antibody were from 1.19×10^{-12}, 4.93×10^{-11} to 1.22×10^{-10} calories. The measurement results were compared to those obtained by a commercially available system. The proposed microcalorimeter has a simple structure and measurement process. The microcalorimeter is also compatible with most polymer-based microfluidic components, which can be applied to various fields of research such as Lab-on-a-chip.

Materials and Methods

Figure 4 shows conceptual and cross-sectional views of the microcalorimeter. The proposed microcalorimeter consists of a thermopile with copper and chrome pairs, one reaction chamber, two reference chambers, and a PDMS microchannel. Details of the

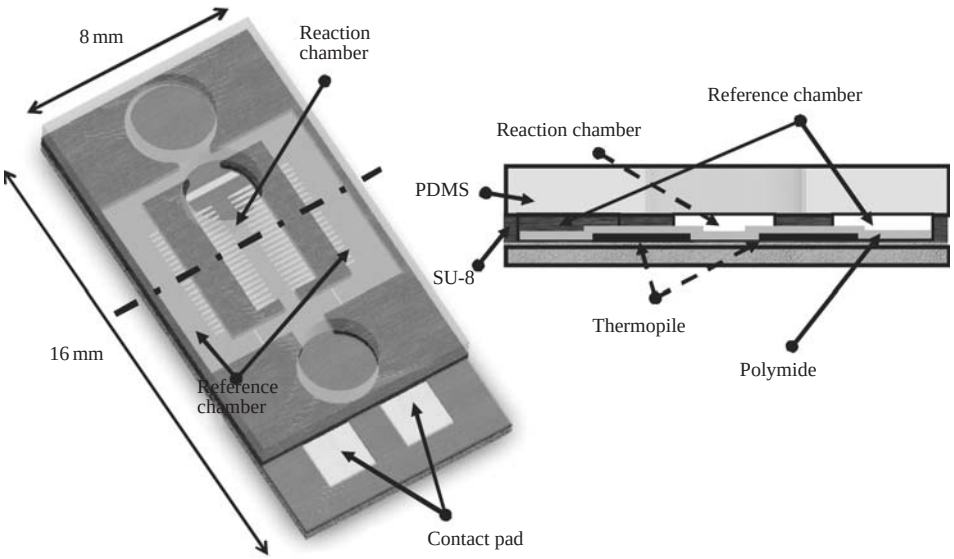

Figure 4. Conceptual and cross-sectional views of the microcalorimeter.

dimensions are as follows: (1) overall dimensions, 16 mm (L) × 8 mm (w); (2) width of the thermopile, 50 μm; (3) length of the thermopile, 2.7 mm; (4) the number of thermocouples, 42; (5) size of the reaction chamber, 5 mm (L) × 3 mm (w) × 300 μm (h); (6) size of the reference chamber, 5 mm (L) × 1 mm (w) × 300 μm (h); (7) thicknesses of the 1st and 2nd SU-8 (SU-8 2100, MicroChem. Corp., USA) layers, 100 μm and 300 μm, respectively; (8) thickness of the chrome and bismuth layer, 1 μm; and (9) thickness of the polyimide layer for insulating the thermopile, 2 μm. Table 2 lists the geometrical parameters.

Table 2. Geometrical parameters of the split-flow microcalorimeter.

Parameter	Dimesion
Overall size	8 mm × 16 mm
Width of the thermopile	50 μm
Length of the thermopile	2.7 mm
Reaction chamber	3 mm × 5 mm × 300 μm
Reference chamber	1 mm × 5 mm × 300 μm

High Thermal Resistivity Layer for Enhancing the Sensitivity of the Microcalorimeter

Thermal energy due to a biochemical reaction is transferred into the air, substrate, and thermal sensing component, simultaneously. To enhance the sensitivity of the sensor, it is important to make a concentrated transfer of the thermal energy into the thermal sensing component, only.

The efficiency of a microcalorimeter is gauged by the dimensionless figure of merit (Z · T), as shown in Eq. 1.

$$Z \cdot T = \frac{S^2 \times \alpha}{k} \cdot T \qquad \text{(Eq. 1)}$$

Z · T: The figure of merit
S: Seebeck coefficient ($V \cdot K^{-1}$ or $V \cdot °C^{-1}$)
α: Electrical conductivity ($\Omega^{-1} \cdot m^{-1}$)
k: Thermal conductivity of the sensor ($W/m \cdot °C$)
T: Temperature (°C)

The Seebeck coefficient (S) and electrical conductivity (α) are 19.97 $\mu V \cdot K^{-1}$ and 1.45×10^7 $\Omega^{-1} \cdot m^{-1}$ in the case of copper and chrome pairs, which are fixed by metal type. And the efficiency of the microcalorimeter (Z) is inversely proportional to the thermal conductivity of the sensor (k). Therefore, the thermal conductivity, which consists of the thermal conductivities of the substrate and PDMS channel, has to be minimized to enhance the efficiency of the microcalorimeter. In this case, since the thermal conductivity of the substrate is much higher than that of the PDMS microchannel (0.15 W/m °C), it is important to reduce the thermal conductivity of the substrate. In this study, the thermal sensing component is thermally isolated from the substrate by using a high thermal resistivity (low thermal conductivity) layer. It is inserted between the thermal sensing component and the substrate layer to reduce a parasitic heat transfer to the substrate. SU-8 is used for the material of the high thermal resistivity layer. Its thermal conductivity of 0.2 W/m °C is much less than that of silicon (130 W/m °C).

The relationship between the rate of parasitic heat transfer to the substrate per temperature change and

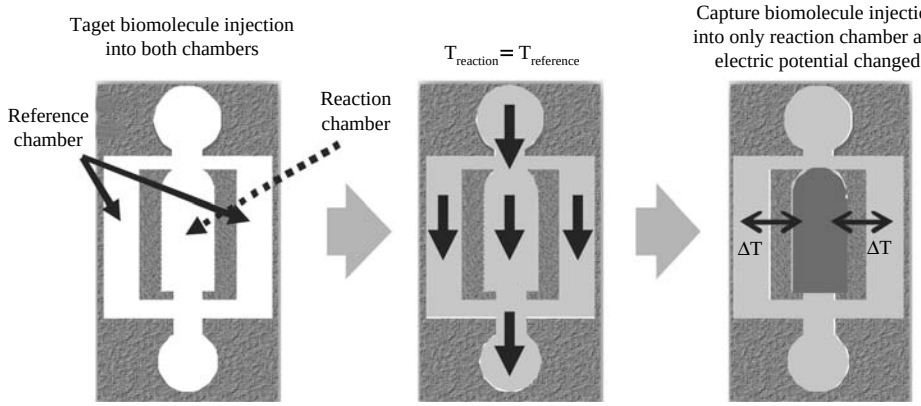

Figure 5. Measurement processes of the split-flow microcalorimeter.

the thermal resistance of the substrate can be expressed using Eq. 2 and Eq. 3[15].

$$R_T = L/(k \cdot A) \quad \text{(Eq. 2)}$$

R_T: Thermal resistance (°C/W)
L : Thickness of a layer (m)
k : Thermal conductivity of a layer (W/m · °C)
A : Area of a layer (m^2)

$$\dot{q} = \frac{q}{\Delta T} = \frac{1}{R_{T1} + R_{T2}} \quad \text{(Eq. 3)}$$

$\dot{q}$: The rate of heat transfer per temperature change (W/°C)
q : The rate of heat transfer (W)
ΔT : Temperature difference (°C)
R_{T1}: Thermal resistance of the SU-8 layer (°C/W)
R_{T2}: Thermal resistance of the silicon substrate (°C/W)

The thicknesses (L) of the silicon substrate and the SU-8 layer are 500 and 100 μm, respectively. The area (A) of each layer is 15 mm^2, which is the same as that of the reaction chamber. Using Eq. 2, the thermal resistances of the SU-8 layer (R_{T1}) and the silicon substrate (R_{T2}) are calculated as 33.33 and 0.26°C /W, respectively. At the same time, the rate of the parasitic heat transfer to the substrate per temperature change is 3.85 W/°C when only a silicon substrate is used. On the other hand, when the SU-8 layer is used for the thermal resistivity layer, the rate of the parasitic heat transfer to the substrate per temperature change is calculated as 0.03 W/°C using Eq. 3. This value is just 0.8% of that when only a silicon substrate is used.

Meanwhile, it is also important to consider the thermal conductivity of the thermal sensing component, the thermopile in this case, for enhancing the sensitivity of the sensor, since a highly thermal conductivity of the thermopile reduces the temperature difference between hot and cold junctions. In this study, the thermopile composed of 56 thermocouples has a width of 50 μm, thickness of 1 μm, and length of 2.7 mm. And its thermal conductivity is about 380 W/m°C. By using these parameters, Eq. 2 and Eq. 3, the thermal resistance of the thermopile can be calculated as 3,350°C/W, and the rate of the heat transfer per temperature change through the thermopile can be calculated as 2.99×10^{-4} W/°C, which is much less than that in the case of the substrate previously mentioned. This means that there is only an insignificant heat transfer thorough the thermopile, so the thermal conductivity of the thermopile is negligible.

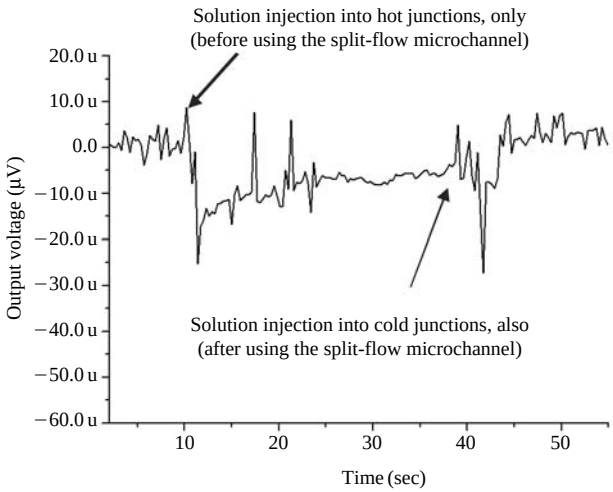

Figure 6. Performance of the split-flow microchannel. Thermal noises due to the solution injection itself are compensated by using the split-flow microchannel. This graph shows the recovery of output voltages to a zero level through the split-flow microchannel.

Principle of the Split-flow Microchannel for Removing an Additional Heating Element

Thermal calibration is an additional step required

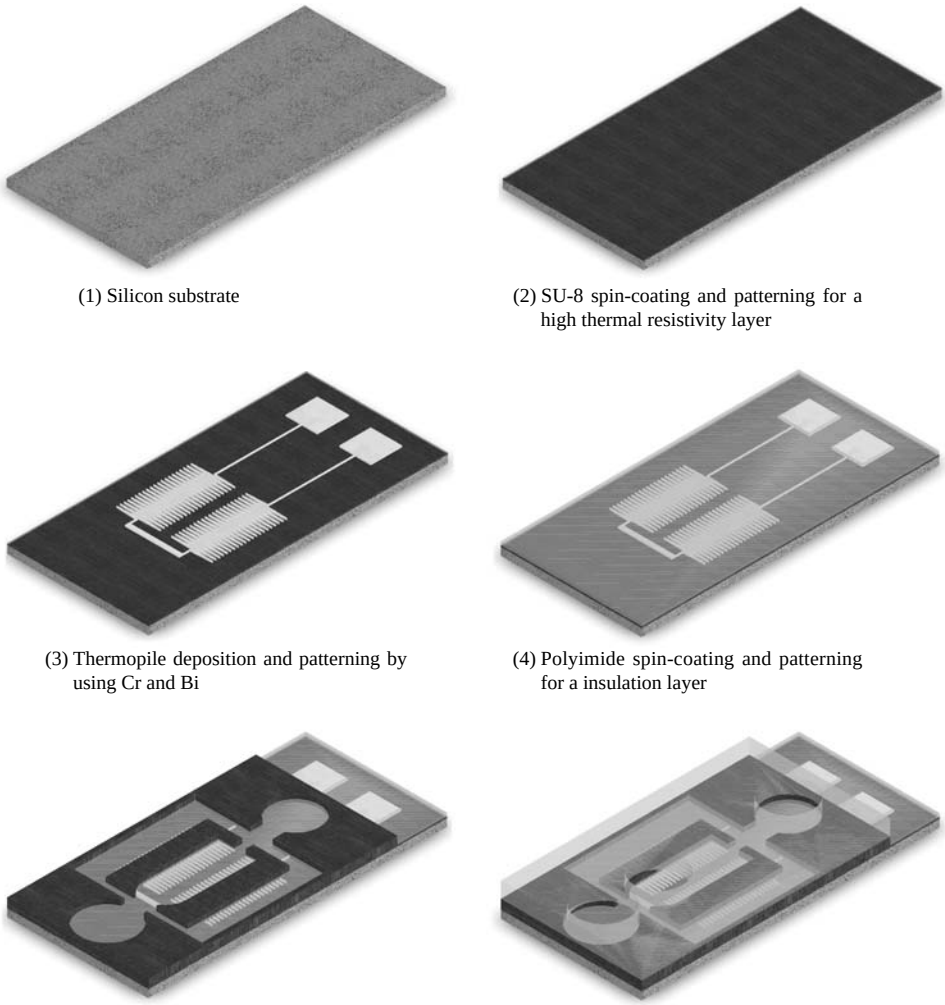

(1) Silicon substrate

(2) SU-8 spin-coating and patterning for a high thermal resistivity layer

(3) Thermopile deposition and patterning by using Cr and Bi

(4) Polyimide spin-coating and patterning for a insulation layer

(5) SU-8 spin-coating and patterning for defining chambers

(6) PDMS channel integration with the thermal components

Figure 7. Simplified fabrication process for the proposed microcalorimeter; 4 masks are required for the fabrication.

for the elimination of thermal noises due to the temperature of the injected solution itself when there is no biochemical reaction. By using the thermal calibration step, only signal changes due to the biochemical reaction can be extracted. Generally, a heater inserted under the hot junctions in the reaction chamber has been used for thermal calibration. When the output voltages are changed not by biochemical reaction, but by the temperature of the solution itself, the heater can compensate the changes. However, a precise heater controller and additional fabrication steps are required for using the heater. In this study, the reference chamber on the cold junctions and the reaction chamber on the hot junctions are integrated within a single chip. Fluidic streams to each chamber are controlled by the split-flow microchannel. The microcalorimeter with the split-flow microchannel can be self-compensated without an additional heating element, which makes the calibration steps no longer required.

Figure 5 shows the measurement processes of the split-flow microchannel without the thermal calibration steps. A fluidic stream containing target biomolecules splits into the reaction and reference chambers through the split-flow microchannel. The temperature of this fluidic stream itself makes the temperatures of the hot and cold junctions the same, and offsets the external noises in both chambers to produce near-zero output voltages. Then, another fluidic stream with the capture biomolecules is applied to the reaction chamber on the hot junctions, only. The applied capture biomolecules produce a reaction heat with the target biomolecules, which produces the temperature differences between the hot and cold junctions. Finally, the voltage due to the biochemical reaction heat in the reaction chamber is measured.

The effect of a split-flow microchannel scheme is demonstrated in Figue 6. It shows that, with an injection of the same solution into each chamber, the output of the proposed microcalorimeter is soon recovered to the zero level. Thermal noises due to the solution injection itself are compensated by using the split-flow microchannel.

Fabrication of the Microcalorimeter with the Split-flow Microchannel

The thermopile is fabricated on the SU-8 layer as a high thermal resistivity material. And the split-flow microchannel is bonded to the thermopile. Figure 7 shows the simplified fabrication process.

First of all, a 100 μm-thick SU-8 layer is spin-coated on a silicon wafer to produce a high thermal resistivity layer. Secondly, a 0.1 μm-thick Cr layer are deposited on the SU-8 layer using a sputtering system and patterned. After this patterning, 1 μm-thick Bi is deposited and patterned as crossed with the Cr patterns. With these metal patterning processes, the thermopile, which is composed of 56 Cr-Bi pairs, is realized. Then, a 2 μm-thick polyimide (PI-2611, DuPont, USA) layer is spin-coated and dried for 6 hours at 95°C. And the polyimide layer is patterned for exposing the contact pads of the thermopile using a reactive ion etcher. After the patterning of the polyimide layer, a 300 μm-thick SU-8 layer is spin-coated. The SU-8 layer is patterned to define the reaction and reference chambers. Lastly, the split-flow microchannel realized by using SU-8 and PDMS is bonded to the substrate with the fabricated thermopile. The overall dimensions of the microcalorimeter with the split-flow microchannel were 16 mm in length and 8 mm in width. Figure 8 shows optical photographs of the fabricated microcalori-meter and its package.

Characterizing the Microcalorimeter through Measurement of Reaction Heat of Biotin and Streptavidin Pairs

In order to verify the characteristics of the fabricated microcalorimeter, generated heat due to the

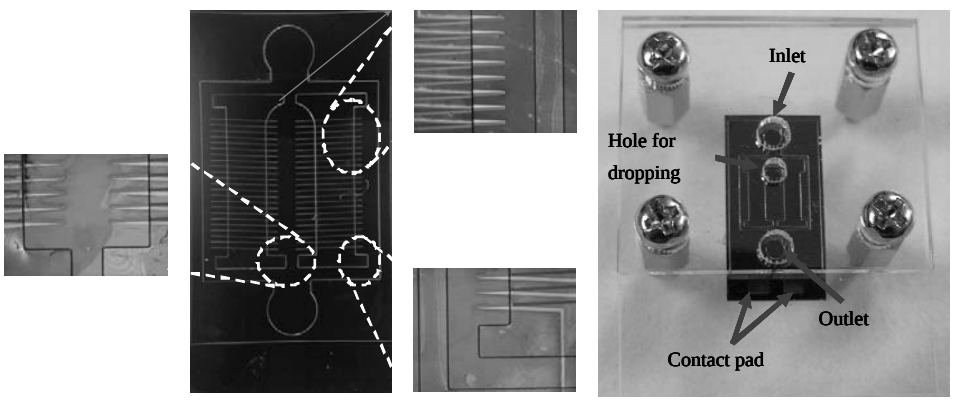

Figure 8. The fabricated microcalorimeter and its package.

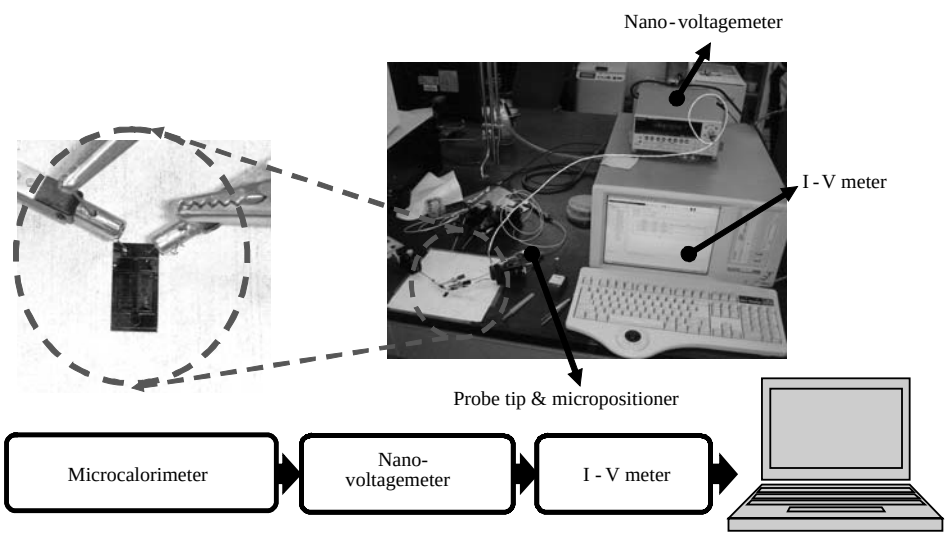

Figure 9. Measurement setup.

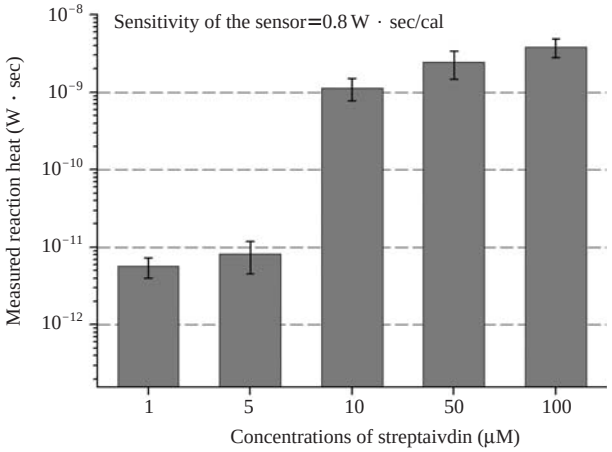

Figure 10. The measured output signals according to the concentration of streptavidin; the sensitivity of the sensor was 0.8 W · sec/cal.

biotin-streptavidin reaction was measured using the sensor. Figure 9 shows the measurement setup.

First, 6 μL of biotin was injected into both chambers at a concentration of 400 μM. Only 3 μL of biotin among the injected solution was applied to the reaction chamber. Then, 3 μL of streptavidin with various concentrations of 1, 5, 10, 50, and 100 μM was applied into the reaction chamber only. Finally, the output signal changes due to the biochemical reaction between the biotin-streptavidin pairs were recorded using a voltage meter (Semiconductor Characterization System 4200, Keithley). The measured output signals of the microcalorimeter ranged from 5.68×10^{-12} to 3.85×10^{-9} W · sec according to the concentrations of streptavidin as shown in Figure 10. By comparing the results with a known reference[16], the output signals per generated heat can be calculated. The calculated output signals, which are the sensitivity of the sensor, were 0.8 W · sec/cal.

Acknowledgements

This work was supported by the Seoul R & BD program and the National Core Research Center (NCRC) of Yonsei University.

References

1. Bruun, L., Koch, C., Jakobsen, M. & Aamand, J. New monoclonal antibody for the sensitive detection of hydroxys-triazines in water by enzyme-linked immunosorbent assay. *Analytica Chimica Acta* **423**, 205-213 (2000).
2. Rattan, A. *et al*. Detection of antigens of Mycobacterium tuberculosis in patients of infertility by monoclonal antibody based sandwiched enzyme linked immunosorbent assay (ELISA), *Tubercle and Lung Disease* **74**, 200-203 (1993).
3. Sen Gupta, R. *et al*. HOPE-Fixation Enables Improved PCR-Based Detection and Differentiation of Mycobacterium tuberculosis Complex in Paraffin-Embedded Tissues. *Pathology Research and Practice* **199**, 619-623 (2003).
4. Dostalek, J., Vaisocherova, H. & Homola, J. Multichannel surface plasmon resonance biosensor with wavelength division multiplexing. *Sensors & Actuators B* **108**, 758-764 (2005).
5. Aoyagi, S. & Kudo, M. Observation of fluorescence-la-beled protein A on a biosensor surface by means of TOF-SIMS. *Sensors & Actuators B* **108**, 708-712 (2005).
6. Gotszalk, T., Grabiec, P. & Rangelowc, I. Quantum size aspects of the piezoresistive effect in ultra thin piezoresistors, Ultramicroscopy **97**, 385-389 (2003).
7. Guan, W., Li, Y., Chen, Y., Zhang, X. & Hu, G. Glucose biosensor based on multi-wall carbon nanotubes and screen printed carbon electrodes. *Biosensors and Bioelectronics* **21**, 508-512 (2005).
8. Ramanathan, K., Khayyami, M. & Danielsson, B. Immunobiosensors based on thermistors. *Affinity Biosensors: Techniques and Protocols* **7**, 19-29 (1998).
9. Beezer, A.E. Biological Microcalorimetry, 311-341 (1980).
10. Werner, W. & Gunther, W.H. Hohne, Chip-calorimeter for small samples. *Thermochimica Acta* **403**, 43-53 (2003).
11. Zhang, Y. & Tadigadapa, S. Calorimetric biosensors with integrated microfluidic channels. *Biosensors and Bioelectronics* **19**, 1733-1743 (2004).
12. Caspary, D., Schropfer, M., Lerchner, J. & Wolf, G. A high resolution IC-calorimeter for the determination of heats of absorption onto thin coatings. *Thermochimica Acta* **337**, 19-26 (1999).
13. Francisco E. Torres. *et al*. Enthalpy arrays, PNAS **10126**, 9517-9522 (2004).
14. Voisard, D., von Stockar U. & Marison, I.W. Quantitative calorimetric investigation of fed-batch cultures of Bacillus sphaericus 1593M. *Thermochimica Acta* **394**, 99-111 (2002).
15. James W. Dally, Packaging of electronic systems. 302-311 (1990).
16. Gonzalez, M. *et al*. Interaction of Biotin with Streptavidin: Thermostability and conformational changes upon binding. *The Journal of Biological Chemistry* **272**, 11288-11294 (1997).